Acta Med. Okayama, 2020
Vol. 74, No. 5, pp. 415–422

Acta Medica Okayama
http://escholarship.lib.okayama-u.ac.jp/amo/

Original Article

Oblique Surface Dose Calculation in High-Energy X-ray Therapy

Naomasa Narihiro[a,c], Masataka Oita[b], and Yoshihiro Takeda[a]*

[a]*Graduate School of Health Sciences, Department of Radiological Technology,*
[b]*Department of Graduate School of Interdisciplinary Sciences and Engineering in Health Systems,*
Okayama University, Okayama 700-8558, Japan,
[c]*Department of Radiological Technology Faculty of Health Science and Technology,*
Kawasaki University of Medical Welfare, Kurashiki, Okayama 701- 0193, Japan

During radiation therapy, incident radiation oblique to the skin surface is high and may cause severe skin damage. Understanding the dose of radiation absorbed by the skin is important for predicting skin damage due to radiation. In this study, we used a high-energy (4 MV) X-ray system and an optically stimulated luminescence dosimeter (OSLD) that was developed for personal exposure dosimetry. We determined the dose variation and angular dependence, which are the characteristics of a small OSLD required to derive the calculation formula for the oblique surface dose. The dose variation was determined using the coefficient of variation. The maximum coefficient of variation for 66 small-field OSLDs was 1.71%. The angular dependence, obtained from the dose ratio of the dosimeter in the vertical direction, had a maximum value of 1.37. We derived a new equation in which the oblique surface dose can be calculated within the error range of −7.7-5.1%.

Key words: optically stimulated luminescent dosimeter, radiotherapy, oblique surface dose, high-energy X-ray therapy, angular dependence

During radiation therapy of breast, head, and neck tumors using high-energy 4-6 megavolt (MV) X-rays, the irradiation must be performed obliquely to the skin surface rather than perpendicularly because of the shape of these body parts. In such oblique exposures, the skin protection effect (which is the main advantage of high-energy X-ray therapy) is lost, and a higher radiation dose is applied to the skin surface [1], which may cause skin damage. Tangential irradiation in which the irradiation angle in breast, head, and neck tumors is obliquely incident on the skin surface increases the skin dose.

Severe dermatitis was reported in 49% of patients undergoing radiation therapy for head and head cancer, and the management of this dermatitis is important [2]. The skin is composed of mainly epidermis and dermis. Most of the skin on the human body has a thickness of 0.1-0.2 cm [3]. As various skin problems appear depending on the buildup of the radiation dose on the skin surface, it is critical to understand the dose during high-energy X-ray therapy in order to predict the occurrence of radiation damage.

For measurements near the skin surface, the charged particle equilibrium is not established; therefore, the measurement accuracy decreases when a Farmer-type ionization chamber dosimeter is used. However, a parallel-plate ionization chamber allows measurements even in regions where charged particle equilibrium is not established, if it is perpendicularly incident on the dosimeter. Gerbi *et al*. investigated the angular dependence of parallel-plate ionization chambers for 6 and

Received March 17, 2020; accepted June 18, 2020.
*Corresponding author. Phone: +81-86-235-6872; Fax: +81-86-222-3717
E-mail: ytakeda@md.okayama-u.ac.jp (Y. Takeda)

Conflict of Interest Disclosures: No potential conflict of interest relevant to this article was reported.

24 MV X-ray beams using a cylindrical ionization chamber and thermoluminescent detectors (TLDs) [1]. They pointed out that parallel-plate ionization chambers depend on both the beam energy and the angle. Regarding the radiation dose near the skin surface, the lower energy absorbed dose becomes a problem. The surface dose also depends on the structure of the accelerator and the electrons scattered from the air on the measurement surface [1], and an accurate calculation of the dose near the skin surface by Monte Carlo simulations requires the head area of the therapeutic device. Accurate information such as the geometrical configuration, shape, and material of each device is required, and it is difficult to obtain an accurate dose calculation because of the complexity of this information. It is also difficult to accurately measure doses < 1 Gy using radiochromic film [4].

Small optically stimulated luminescence dosimeters (OSLDs) that are designed for personal exposure dosimetry [5-9] have been used for both individual dose measurements and diagnostic X-ray dose measurements [10, 11]. Small OSLDs have recently been used for dosimetry in the field of radiotherapy [12-19]. Their accuracy is within ± 1% of the absorbed dose measured by a ionization chamber dosimeter with uncertainties of 1-2% (1σ) [12]. Small OSLDs have also been used for measuring absorbed doses in the areas of brachytherapy [20-22] and proton therapy [23]. In radiation therapy, various measurements using small OSLDs have been reported, but there has been no report in which the calculation formula was derived from the measured values of the oblique surface dose using a small OSLD. In the present investigation, we measured the oblique surface dose using high-energy (4 MV) X-rays and a small OSLD. We then used the results to derive an equation for calculating this oblique surface dose.

Materials and Methods

nanoDot® OSLD. A small nanoDot® OSLD (Nagase-Landauer, Tsukuba, Japan) was used. This dosimeter consists of a sheet-like carbon-added α-aluminum oxide (α-Al_2O_3: C) covered with polyethylene; it is a circular element (0.5 cm dia., 0.03 cm thick), and it is shielded from light by a 1 × 1 × 0.2 cm case (Fig. 1). As the serial number and barcode are displayed on the light-shielding case, individual dosimetry management is possible. Prior to its use, the device is removed from the light-shielding case, annealed, and returned to the case. The reading device used was a microStar® from Nagase-Landauer. The advantage of the nanoDot OSLD is that it can be read out multiple times and can be reused after a measurement if it is annealed (Fig. 2). A 20-h-long annealing is necessary when a high radiation dose is applied to the dosimeter during radiation therapy [16]. In this study, the annealing was performed for more than 24 h. We used a high-energy X-ray irradiator (Linac Primus-KD2, Siemens, Berlin, Germany) and a Solid Water phantom (Toyo Medic Co., Tokyo) with a density of 1.04 g/cm^3 and the dimensions 40 × 40 × 20 cm.

The characteristics of the nanoDot OSLD include dose-response, dose rate dependence, energy dependence, dose variation, angular dependence, and fading. We examined the dose variation and angular dependence required of the nanoDot OSLD for measuring

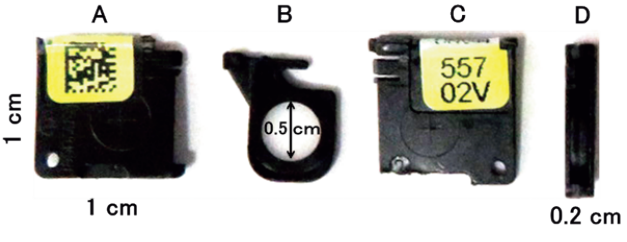

Fig. 1 Structure of the nanoDot OSLD. **A**, Barcode side; **B**, Interior; **C**, ID side; **D**, Cross-section. The dosimeter disk (0.5 cm dia., 0.03 cm thick) covered with sheet-like carbon-added α-aluminum oxide (α-Al_2O_3: C) with polyethylene is shielded from light in a 1 × 1 × 0.2 cm shading case. The serial number and barcode are displayed on the shading case.

Fig. 2 Measurement cycle. The nanoDot OSLD can be read multiple times; after measurement, annealing can be repeated as many times as necessary.

oblique surface doses. We then measured the oblique surface dose and derived the equation for the oblique surface dose from the results.

Dose variation. A total of 66 nanoDot OSLDs were placed on a Solid Water phantom and irradiated simultaneously (Fig. 3) with 4 MV X-ray radiation. We used a dose rate of 200 MU/min, a source-chamber distance (SCD) of 100 cm, an irradiation field of 40×40 cm, and a monitor unit value of 200 MU. The linac was correctly calibrated by the monitor dosimeter, with a maximum dose of 1 cGy per 1 MU. Therefore, when 200 MU is irradiated, the surface dose is <200 cGy, which is a good dose-response range.

Considering the signal loss immediately after irradiation, the readout was performed 30 min after irradiation. It is often reported that the optimal number of reads per piece is three [5,13,17]. OSLDs can be read multiple times, and Reft *et al.* reported that multiple readings of measurements can reduce statistical errors [18]. We performed 10 readings, excluded the maximum and minimum values, and averaged the remaining 8 readings. The dose variation was evaluated using the coefficient of variation (CV).

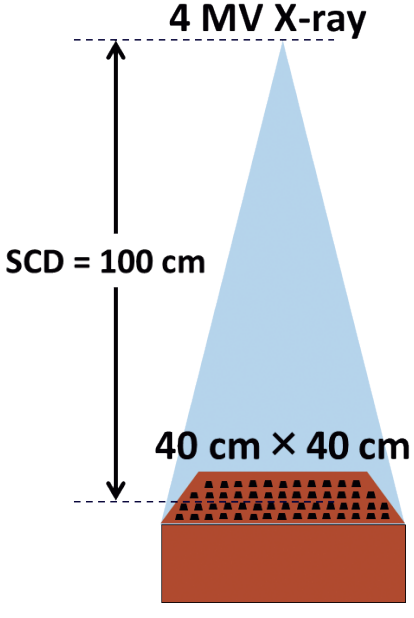

Fig. 3 A total of 66 small OSLDs were placed on the Solid Water phantom and irradiated simultaneously. The X-ray irradiation energy was 4 MV, the dose rate 200 MU/min, the distance between the source and dosimeters was 100 cm, the irradiation field was 40 × 40 cm, and the monitor unit value was 200 MU.

Angular dependence. Irradiation was performed without any scattered radiation around the nanoDot OSLD. The nanoDot OSLD was set on a thin piece of styrofoam (0.5 cm thick, 1 cm wide, 10 cm long) fixed to the linac bed. The vertical angle to the barcode surface of the nanoDot OSLD was set to 0° (Fig. 4A,B). Irradiation was performed from 24 directions in 15° increments from 0° to 345° in the gantry angle of the linac.

After irradiation, readings were taken 10 times in the same manner as the measurement of dose variation, and the measured value was taken as the average value of 8 of these readings, excluding the max. and min. values. In addition, the barcode surface of the nanoDot OSLD was rotated 90° to the right (Fig. 4C,D), irradiation was performed from 24 directions, and the ratio of the dose at each angle to that at 0° was calculated. We then created a single chart by combining the measurement results in the A-B and C-D directions.

Oblique surface dose. The nanoDot OSLD was embedded in the surface of the Solid Water phantom (Fig. 5). The thickness of the nanoDot OSLD is 0.2 cm, and the circular element is installed in the center; therefore, the surface dose in this study was 0.1 cm. The irradiation was performed in 11 configurations for various lengths of the square irradiation fields (2,3,4,5,6,8,10,15,20,25, and 30 cm), resulting in a total of 66 combinations. We used the same experimental parameters and measurement methods for as those used for observing the dose variation. The incident direction of the nanoDot OSLD was taken from the

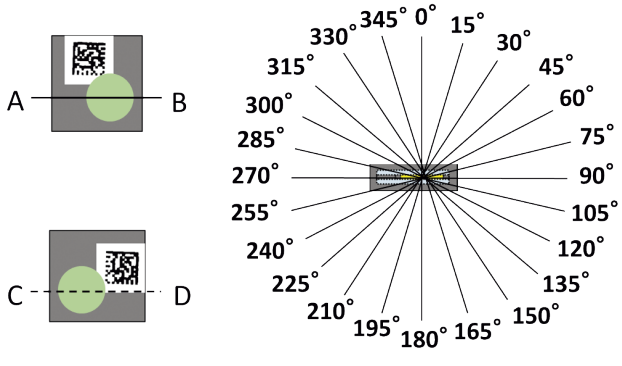

Fig. 4 The vertical angle to the barcode surface of nanoDot OSLD was set to 0°. Irradiation was performed from 24 directions at 15° intervals from 0° to 345° in the gantry angle of the linac. Similarly, the bar code surface of the nanoDot OSLD was rotated 90° to the right and irradiation was performed from 24 directions.

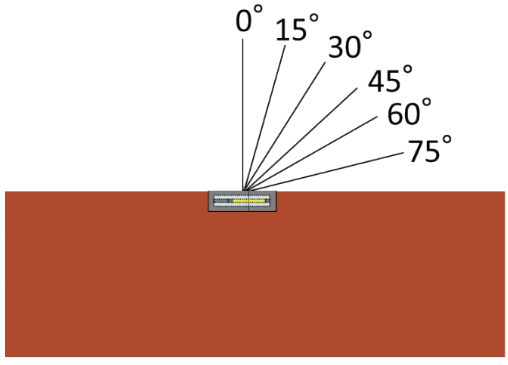

Fig. 5 A nanoDot OSLD was embedded in the surface of the Solid Water phantom. Irradiation was performed in 11 ways with one side of the square irradiation field measuring 2, 3, 4, 5, 6, 8, 10, 15, 20, 25, or 30 cm. A total of 66 irradiation combinations were performed.

A-B direction, and the measured values were corrected for the angular dependence of the dosimeter to determine the absorbed dose per MU. The measured value was divided by the monitor unit value of 200 MU to obtain the surface dose (cGy) per MU. The dose ratio for an irradiation angle of 0° was obtained for each irradiation field.

Oblique surface dose calculation. Using the results obtained as described above, we calculated the surface dose per MU and derived an equation to calculate the oblique surface dose using a two-dimensional polynomial. The dose obtained using this equation is the absorbed dose at a depth of 0.1 cm at the center of the irradiation field of the 4 MV X-ray. Using the calculation formula, we performed the calculations under the same conditions as those used when we measured the nanoDot OSLD, and we calculated the error of the calculated value with respect to the measured value.

Results

Dose variation. The CVs for the 66 nanoDot OSLDs configurations are presented in Fig. 6. The CVs were calculated from the average values and standard deviations according to the previous formula. The average of the 66 CVs was 1.00%, the minimum was 0.33%, and the maximum was 1.71%.

Angular dependence. Fig. 7 shows the angular dependences of the nanoDot OSLD in the A-B and C-D directions obtained by turning the barcode surface 90° clockwise. The vertical angle to the bar code surface of the nanoDot OSLD was 0°, and the gantry angle of the linac was varied from 0° to 345° in 15° increments. From the measured values, the dose ratio of each angle measurement to the base value at 0° was calculated. The maximum dose ratio was 1.32 at 255° in the A-B direction and 1.37 at 105° in the C-D direction. All dose ratios were 1.00 or higher. The variation trends in the A-B and C-D directions were similar. The angular dependence tended to be large in directions parallel to the dosimeter plane at 90° or 270°.

Oblique surface dose. In Fig. 8, the horizontal axis shows the length (cm) of a square field, and the

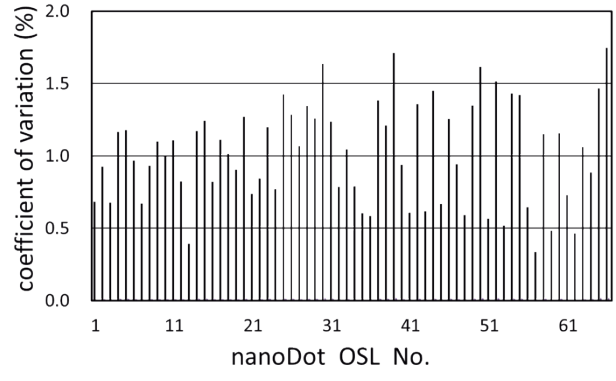

Fig. 6 Coefficient of variation (CV) of the 66 small OSLDs used. This was calculated from the mean and standard deviation of 8 readings after excluding the maximum and minimum values of the ten readings. The average CV for the 66 OSLDs was 1.00%, with a min. value of 0.33% and a max. value of 1.71%.

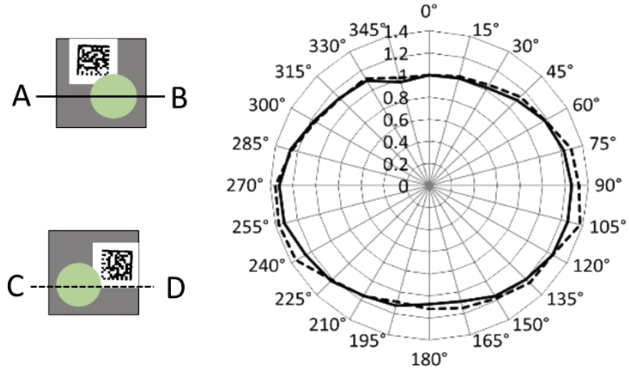

Fig. 7 Angular dependence of the nanoDot OSLD in the A-B direction and the C-D direction when the barcode surface is rotated 90° to the right. The nanoDot OSLD was irradiated at 15° intervals from the 0° to 345° linac gantry angles with a vertical angle of 0° with respect to the barcode surface. The angular dependence was evaluated from the dose ratio of each angle to the measured value in the 0° direction.

vertical axis shows the oblique surface dose relative to the dose of a gantry angle of 0° and a field of 10 × 10 cm. All doses were corrected for the angular dependence. As the relative values of 0°, 15°, 30°, 45°, 60°, and 75° with respect to 0° are 1.00, 1.02, 1.05, 1.13, 1.18, and 1.29, respectively, the angle-dependent correction values are 1.00, 0.98, 0.95, 0.88, 0.85, and 0.78, respectively. For all angles from 0° to 75°, the relative dose increased with the angle. In addition, the relative dose increased with the increase in the irradiation field. The increase was steeper as the oblique angle increased.

The surface doses (cGy) per MU are listed in Table 1. The surface dose is the quotient of the measured value divided by the monitor unit value of 200 MU. As shown in Fig. 8, the surface dose increased with the irradiation field, resulting in an increase in the oblique dose. The dose per MU for a 5-cm-long square perpendicular to the surface was 0.39 cGy, which was the minimum measured dose. The maximum value of the measured dose was 0.81 cGy for one piece of the square field 20 cm and 25 cm and an oblique angle of 75°.

Table 2 shows the dose ratio for an irradiation angle of 0°. At an incidence angle of 75°, the dose ratios were 1.65 and 1.21 for one piece of the square field 5 cm and 30 cm , respectively. Thus, the smaller the irradiation field is, the larger the increase in the dose is with the irradiation angle.

Oblique surface dose calculation. A two-dimensional polynomial was fitted to the surface dose per the MU values listed in Table 1 by the least-squares method. The derived oblique surface dose calculation Equation (1) and parameters are listed in Table 3.

$$z=(z_0+A_1x+A_2x^2+A_3x^3+A_4x^4+A_5x^5+B_1y+B_2y^2+B_3y^3+B_4y^4+B_5y^5)\times MU \quad (1)$$

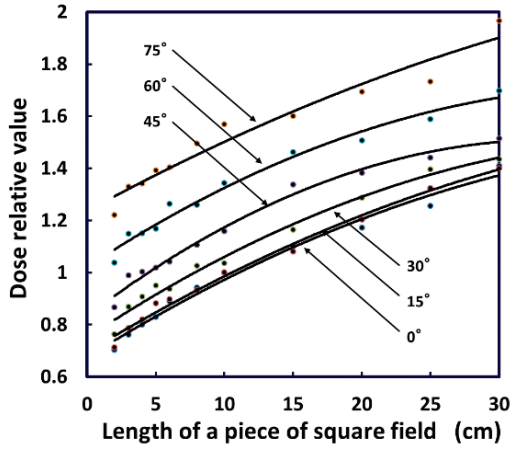

Fig. 8 Dose relative value vs. square irradiation field. The horizontal axis is the length of a square field piece (cm), and the vertical axis is the relative value of the oblique surface dose with respect to the dose delivered at gantry angle of 0° to an irradiation field with an area of 10 × 10 cm. All doses are angle-dependent corrected.

Table 1 Surface dose per MU (cGy)

Length of a piece of square field (cm)	Irradiation angle (degree)					
	0	15	30	45	60	75
5	0.39	0.39	0.42	0.47	0.54	0.64
10	0.45	0.46	0.49	0.54	0.61	0.70
15	0.51	0.52	0.55	0.60	0.67	0.76
20	0.56	0.57	0.60	0.65	0.72	0.81
25	0.61	0.61	0.63	0.67	0.73	0.81
30	0.65	0.65	0.65	0.67	0.72	0.79

Table 2 Dose ratio at radiation incidence of 0°

Length of a piece of square field (cm)	Irradiation angle (degree)					
	0	15	30	45	60	75
5	1.00	1.02	1.10	1.23	1.41	1.65
10	1.00	1.03	1.10	1.21	1.36	1.55
15	1.00	1.02	1.08	1.18	1.32	1.49
20	1.00	1.01	1.07	1.16	1.28	1.45
25	1.00	1.00	1.03	1.10	1.20	1.34
30	1.00	1.00	1.00	1.03	1.10	1.21

Table 3 Parameters for calculating the surface dose

Z_0	0.28848
A_1	0.02949
A_2	−0.00233
A_3	1.55E-04
A_4	−5.08E-06
A_5	5.96E-08
B_1	1.55E-04
B_2	1.05E-05
B_3	1.04E-06
B_4	−1.41E-08
B_5	7.10E-11

Table 4 Calculated oblique surface dose [cGy] per MU and measured using nanoDot OSLD

Field (cm)	Irradiation angle (degree)											
	0		15		30		45		60		75	
	M	C (e)	M	C (e)	M	C (e)	M	C (e)	M	C (e)	M	C (e)
5	0.39	0.39 (0)	0.39	0.40 (2.6)	0.42	0.43 (2.4)	0.47	0.47 (0)	0.54	0.54 (0)	0.64	0.63 (−1.6)
10	0.45	0.46 (2.2)	0.46	0.47 (2.2)	0.49	0.49 (0)	0.54	0.54 (0)	0.61	0.60 (−1.6)	0.70	0.69 (−1.4)
15	0.51	0.52 (2.0)	0.52	0.53 (1.9)	0.55	0.55 (0)	0.60	0.60 (0)	0.67	0.66 (−1.5)	0.76	0.75 (−1.3)
20	0.56	0.57 (1.8)	0.57	0.57 (0)	0.60	0.60 (0)	0.65	0.64 (−1.5)	0.72	0.71 (−1.4)	0.81	0.80 (−1.2)
25	0.61	0.59 (−3.3)	0.61	0.60 (−1.6)	0.63	0.63 (0)	0.67	0.67 (0)	0.73	0.74 (1.4)	0.81	0.83 (2.5)
30	0.65	0.60 (−7.7)	0.65	0.61 (−6.2)	0.65	0.64 (−1.5)	0.67	0.68 (1.5)	0.72	0.75 (4.2)	0.79	0.83 (5.1)

Field, Length of a piece of square field; M, measured value (cGy); C, calculated value (cGy); (e), error (%).

where z represents the oblique surface dose (cGy), x is the length of a piece of square field (cm), y is the irradiation angle (degree), and MU is the monitor unit value. ($R^2 = 0.9896$).

Table 4 shows the oblique surface dose per MU calculated using this derived equation and the values measured using the nanoDot. The errors of the calculated value with respect to the measured values are shown. The error range was −7.7-5.1%. The error was large when one piece of the square field was 30 cm.

Discussion

Characteristics of the OSLD. The characteristics of a nanoDot OSLD include dose-response, dose rate dependence, energy dependence, dose variation, angular dependence, and fading. Here, we examined the dose variation and angular dependence required for the characteristics of the nanoDot OSLD for the measurement of oblique surface doses. We will first discuss four characteristics.

A good dose range for the dose-response of the nanoDot OSLD is 50-200 cGy [17-19], and in the present experiment, the dose range was 78-158 cGy; therefore, all of the measurements were within the well-linearized dose range. The nanoDot OSLD shows good dose-rate dependence agreement with the ionization chamber dosimeters in the range of 100-500 cGy/min [13, 14]. As the dose rate in the present experiment was 200 cGy/min, it was not necessary to consider the dose rate dependency.

The energy of the nanoDot OSLD does not depend on the photon energy in the 6-18 MV range [12, 13]. In our present experiment, a reader calibrated with 4 MV X-ray energy was used and only 4 MV X-ray energy was used; thus, there is no need to consider the energy dependence. It has been reported that in the dose range 50-400 cGy, the nanoDot OSLD signal shows a sharp decay immediately after irradiation and then stabilizes after approx. 8 min [18]. Compared to 1000 cGy, the dose 100 cGy has a significant signal loss at 10 min post-irradiation, and the signal loss is reported to be dose-dependent [17]. An investigation of the suitability of using an OSLD for radiation therapy took some measurements 30 min after irradiation [15]. The doses measured in our study were in the range 78-158 cGy and were read 30 min after irradiation. It is thus not necessary to consider the signal loss.

Dose variation. The nanoDot OSLD measures with high reproducibility, and the CV for 40 samples is reported to be 1.5% [16]. The average value of the CV of the 66 nanoDot OSLDs used herein was 1.00%, and the maximum value was 1.71%. The CV is usually < 2% [9]. The CV obtained for ten readings of one nanoDot OSLD was reported to be 1.33% [9], but the average of the 66 CVs we measured was 1.00%. From the above results, we consider that the 66 nanodot OSLDs used in this study have high reproducibility and can be operated with high accuracy.

Angular dependence. Angular dependence is observed in both the A-B and C-D directions of the nanoDot OSLD. Regarding the angular dependence of the dosimeter surface, a slight difference is observed even in the vertical direction of 0° (barcode surface) and 180° (ID surface), and the angular dependence increases around 90° and 270° (Fig. 7). This is due to the shape of the nanoDot OSLD. The nanoDot OSLD has a circular element that is 0.03 cm thick and 0.5 cm in diameter, covered in a thin polyester case measuring $1 \times 1 \times 0.2$ cm. The increased angular dependence from the horizontal rather than the vertical is due to the generation of secondary electrons from the polyester case.

Because the thickness in the vertical direction of the polyester case is smaller than the thickness in the horizontal direction, the generation of secondary electrons is small. In addition, the dose varies slightly between 90° and 270° horizontally. The cause is assumed to be that the element is not located at the center of the polyester case, as shown in Fig. 1.

Kerns *et al.* [5] reported that irradiating a nanoDot OSLD from 90° and 270° reduced the response compared to irradiation with an incident beam normal to the plane of the dosimeter by 4% at 6 MV and 3% at 18 MV. They installed a nanoDot OSLD on a phantom and measured the angular dependence. As our measurements were made in air, they were affected by low-energy components. We believe that the measurements in the phantom differed from our results due to the presence of high-energy components.

Oblique surface dose. The radiation contribution to the surface dose is related mainly to the structure of the accelerator, the electrons scattered from the air on the surface, and the dose from the lower surface. The measurements in this study included all of these factors. As shown in Table 2, at the radiation incidence angles from 0° to 75°, the relative dose increased with the angle, with a rate of change proportional to the angle. Further, the relative value of the dose increased when the irradiation field increased. This was due to the increase in the generation of secondary electrons.

Whether it is a high-energy X-ray or a scattered component, the dose that contributes to the surface dose is considered to be the absorbed dose due to the low-energy secondary electrons. Considering only low-energy secondary electrons, this can be explained using a simple model. Fig. 9 presents an explanatory diagram using Kernel, which is a three-dimensional spread of secondary electrons generated from a monochromatic photon beam. Here, Kernel is shown for three X-rays (A, B, and C) of the irradiation field incident on the surface. The incident point B is the center of the irradiation field. The higher the energy of the Kernel, the more it spreads forward.

In the case of high-energy (4 MV) X-rays normally incident on the surface, the Kernel spread is maximum at a depth of 1 cm from the point of incidence. The same applies to the case of oblique incidence, where the maximum is at a depth of 1cm from the incident point; however, the Kernel spread shows a shallow region. For oblique incidence, the dose contribution at the center of the irradiation field is not given by the X-ray contribution from point B, but by the contribution from point C.

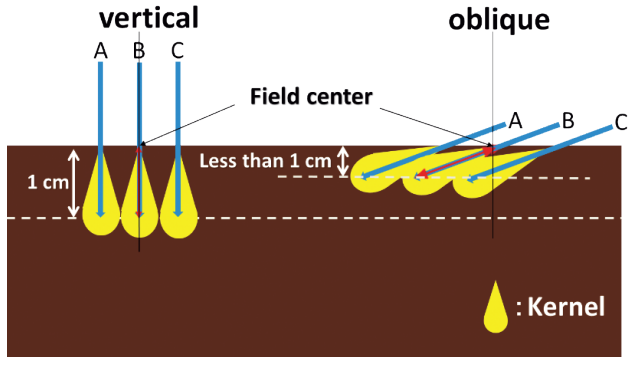

Fig. 9 Explanatory diagram using Kernel for the case of normal incidence on the surface and the case of oblique incidence. The Kernel for the cases when three X-rays (A, B, and C) of the irradiation field are incident on the surface, with B being the center of the irradiation field.

Oblique surface dose calculation. We have found no published studies that calculate oblique surface doses using nanoDot OSLDs. In this study, we calculated Eq. (1) to obtain the oblique surface dose. If a calculation formula program is developed, the surface dose can be easily calculated by providing three inputs: the square irradiation field dimension, the irradiation angle, and the MU value. If the total MU value of all of the treatment periods is provided as input, then the total surface dose that the patient receives from the incident radiation direction can be calculated. However, as summarized in Table 4, the error range is −7.7-5.1%. At any angle, the error increased when one side of the square field was 30 cm. Thus, the formula should be used with this error in mind. We believe that our proposed formula can help radiation therapy practitioners in estimating radiation levels that would not produce irreparable skin damage in patients.

We did not compare this new method with standard methods such as Monte Carlo simulations and parallel plate ionization chamber measurements in the present study. However, the nanoDot OSLD is easy to use and enables high-accuracy measurements with minimal setup time. Its accuracy, when used for radiation therapy purposes, is within ±1% between the absorbed doses measured by the OSLD and the ionization chamber dosimeter; in addition, its uncertainty is 1-2% (1σ) [12]. OSLDs were originally developed for personal

exposure dosimetry. They are now also used for X-ray diagnostic dosimetry measurements. For example, in a recent study, a nanoDot OSLD was actually placed directly on the skin surface of a patient and measurements were conducted [15]. It is expected that the use of OSLDs in dosimetry will further increase in the fields of brachytherapy and particle therapy.

In conclusion, we derived a new equation for calculating oblique surface doses of 0.1 cm depth using high-energy 4 MV X-ray and the nanoDot OSLD. The error range was −7.7-5.1% by comparing the value obtained from the calculation formula with the measured value of the nanoDot OSLD.

References

1. Gerbi BJ, Meigooni AS and Khan FM: Dose buildup for obliquely incident photon beams. Med Phys (1987) 14: 393–399.
2. Giro C, Berger B and Bolke E: High rate of severe radiation dermatitis during radiation therapy with concurrent cetuximab in head and neck cancer: Results of a survey in EORTC institutes. Radiotherapy Oncology (2009) 90: 166–171.
3. Tortora GJ and Derrickson B: Principles of Anatomy and Physiology, 13 th edition. Biological Science Textbooks (2012).
4. Chełminski K, Bulski W, Georg D, Bodzak D, Maniakowski Z, Oborska D, Rostkowska J and Kania M: Energy dependence of radiochromic dosimetry films for use. Rep Pract Oncol Radiother (2010) 15: 40–46.
5. Kerns JR, Kry SF, Sahoo N, Followill DS and Ibbott GS: Angular dependence of the nanoDot OSL dosimeter. Med Phys (2011) 38: 3955–3962.
6. Edmund JM: Effects of temperature and ionization density in medical luminescence dosimetry using Al_2O_3: C. Risø National Laboratory Technical University of Denmark, Roskilde, Denmark (2007).
7. Jursinic PA: Characterization of optically stimulated luminescent dosimeters, OSLs, for clinical dosimetric measurements. Med Phys (2007) 34: 4594–4604.
8. Al-Senan RM and Hatab MR: Characteristics of an OSLD in the diagnostic energy range. Med Phys (2011) 38: 4396–4405.
9. Yahnke CJ: MicroStar InLight Systems (2009) Rev. 2, June 10.
10. Takegami K, Hayashi H, Okino H, Kimoto N, Maehata I, Kanazawa Y, Okazaki T and Kobayashi I: Practical calibration curve of small-type optically stimulated luminescence (OSL) dosimeter for evaluation of entrance skin dose in the diagnostic X-ray region. Radiol Phys Technol (2015) 8: 286–294.
11. Tappouni R and Mathers B: Scan quality and entrance skin dose in thoracic CT: A comparison between bismuth breast shield and posteriorly centered partial CT scans. ISRN Radiol (2013) 2013: 1–6.
12. Yukihara EG, Mardirossian G, Mirzasadeghi M, Guduru S and Ahmad S: Evaluation of Al2O3: C optically stimulated luminescence (OSL) dosimeters for passive dosimetry of high-energy photon and electron beams in radiotherapy. Med Phys (2008) 35: 260–269.
13. Viamonte A, da Rosa LAR., Buckley LA, Cherpak A and Cygler JE: Radiotherapy dosimetry using a commercial OSL system. Med Phys (2008) 35: 1261–1266.
14. Schembri V and Heijmen BJM: Optically stimulated luminescence (OSL) of carbon-doped aluminum oxide for film dosimetry in radiotherapy. Med Phys (2007) 34: 2113–2118.
15. Yusof FH, Ung NM, Wong JHD, Jong WL, Ath V, Phua VCE, Heng SP and Ng KH: On the use of optically stimulated luminescent dosimeter for surface dose measurement during radiotherapy. PLOS ONE (2015) 10: e0128544.
16. Poirier Y, Kuznetsova S and Villarreal-Barajas JE: Characterization of nanoDot optically stimulated luminescence detectors and high-sensitivity MCP-N thermoluminescent detectors in the 40–300 kVp energy range. Med Phys (2018) 45: 402–413.
17. Omotayo AA, Cygler JE and Sawakuchi GO: The effect of different bleaching wavelengths on the sensitivity of Al2O3: C optically stimulated luminescence detectors (OSLDs) exposed to 6 MV photon beams. Med Phys (2012) 39: 5457–5468.
18. Reft CS: The energy dependence and dose response of a commercial optically stimulated luminescent detector for kilovoltage photon, megavoltage photon, and electron, proton, and carbon beams. Med Phys (2009) 36: 1690–1699.
19. Jursinic PA: Changes in optically stimulated luminescent dosimeter (OSLD) dosimetric characteristics with accumulated dose. Med Phys (2010) 37: 132–140.
20. Tien CJ, Ebeling R, Hiatt JR, Curran B and Stemick E: Optically stimulated luminescent dosimetry for high dose rate brachytherapy. Radiat Oncol (2012) 2: 1–7.
21. Andersen CE, Nielsen SK, Greilich S, Helt-Hansen J, Lindegaard JC and Tanderup K: Characterization of a fiber-coupled Al2O3: C luminescence dosimetry system for online in vivo dose verification during 192 Ir brachytherapy. Med Phys (2009) 36: 708–718.
22. Brodin NP, Mehta KJ, Basavatia A, Goddard LC, Fox JL, Feldman SM, McEvoy MP and Tomé WA: A skin dose prediction model based on in vivo dosimetry and ultrasound skin bridge measurements during intraoperative breast radiation therapy. Int Multidiscip J Brachytherapy (2019) 18: 720–726.
23. Kerns JR, Kry SF and Sahoo N: Characteristics of optically stimulated luminescence dosimeters in the spread-out Bragg peak region of clinical proton beams. Med Phys (2012) 39: 1854–1863.